ELSEVIER

www.elsevier.nl/locate/jorganchem

Journal of Organometallic Chemistry 609 (2000) 53–59

Journal of Organometallic Chemistry

An 'atoms in molecules' (AIM) analysis of the dihydrogen bond in organometallic compounds

Maria José Calhorda [a,b,*], Pedro E.M. Lopes [a]

[a] *Instituto de Tecnologia Química e Biológica (ITQB), Quinta do Marquês, EAN, Apt 127, 2781-901 Oeiras, Portugal*
[b] *Departamento de Química e Bioquímica, Faculdade de Ciências da Universidade de Lisboa, 1749-016 Lisbon, Portugal*

Received 19 February 2000; accepted 14 April 2000

Abstract

The interactions of the Ir–H···H–X type (X = O, N) were studied theoretically in models of the neutral complex $[Ir(H)_3(PPh_3)(C_5H_4NHR]$ and the two cationic derivatives *cis*-$[IrH(OH)(PMe)_4][PF_6]$ and $[IrH_2(CO)(PPh_3)_2(pzH–N)][BF_4]$. The geometries were optimized using both RHF and MP2 calculations and an analysis of the charge density was carried out with the atom in molecules (AIM) procedure. The conclusion was that a hydrogen bond between the hydride and the protonic hydrogen is found only in the neutral complex. In the cationic species, the counterion is determining in order to get a good agreement between the optimized and the X-ray determined structures, and the short H···H distance is a consequence. The only hydrogen bonds appear to be formed between hydrogen atoms and fluorine atoms of the anion.

Keywords: Hydrogen bonds; Metal hydrides; AIM; Ab initio calculations

1. Introduction

In recent years, a new type of hydrogen bond, called the dihydrogen bond by Crabtree et al. [1], was found to be present in many structures of organometallic hydride complexes. There is a short H···H distance, between a metal hydride and a proton bound to an electronegative atom, in a M–H···H–X arrangement. The first example, *cis*-$[IrH(OH)(PMe)_4][PF_6]$, was published in 1986 [2a] and a neutron diffraction structural study appeared a few years later, showing a short O–H···H–Ir distance of 2.40(1) Å and an Ir–O–H angle of 104.4(7)° [2b]. The same O–H···H–Ir group was detected by NMR, with an estimated H···H distance of 1.8 Å, in the complex $[Ir(H)_2L'(PPh_3)_2][SbF_6]$, where L′ is the iminol form of quinoline-8-acetamide (the hydrogen atoms were not located in the structure) [3]. The related N–H···H–Ir arrangement was found in a related complex of 2-aminopyridine (L), $[Ir(H)_3(PPh_3)_2L]$ [4] and more examples from other authors followed [5]. Attempts at obtaining an intermolecular hydrogen bond of the same kind were successful [6], the first example being observed in the product of cocrystallization of $ReH_5(PPh_3)_3$ with indole. A neutron diffraction structure showed that two of the hydrides were interacting with the N–H bond of the indole (H···H distances 1.75 and 2.25 Å) [6a]. After the initial novelties, much work in the field followed, including reviews [7], and works containing structural analyses based on data from the Cambridge Crystallographic Data Base (CSD) [8] were published [9]. Theoretical studies were performed in order to understand the nature of these weak hydrogen bonds, based on several types of methods [4b,6a,e,f,7a,b,9b,10–12]. In a previous work, we analyzed both inter [10] and intramolecular hydrogen bonds [11] involving the M–H bond, taking the structures from the CSD, and performed theoretical calculations. Although most of the complexes exhibiting short intramolecular H···H contacts analyzed are cationic, some are neutral, and a comparative analysis could be made, leading us to the conclusions that the counterion plays a major role in determining the structure of the cation and there was no unambiguous evidence about the existence of a hydrogen bond. In this work, we go back to the relevant compounds [2,6,11,13], perform

* Corresponding author. Fax: +351-21-4411277.
E-mail address: mjc@itqb.unl.pt (M.J. Calhorda).

0022-328X/00/$ - see front matter
PII: S0022-328X(00)00235-7

RHF and MP2 calculations [14], more reliable for the study of weak interactions where dispersion forces may be important [15], and analyze the results using the formalism of AIM (atoms in molecules) [16].

2. Results and discussion

2.1. Structures and models

In our previous study of hydrogen bonds of the type M–H···H–X [11], we analyzed, in detail, the bonding on models for two cationic complexes, *cis*-[IrH(OH)-$(PMe)_4$][PF_6] [2], and [$IrH_2(CO)(PPh_3)_2$(pzH–N)][BF_4]-[C_6H_5Me] [13], and compared it with the results of a study of [$Ir(H)_3(PPh_3)_2(C_5H_4NHR)$] [4b]. The DFT calculations [17] were performed with the ADF program [18] and a good agreement between experimental and calculated geometry was found. In this work, we want to use the AIM formalism to interpret the bonds between atoms, and the available programs [19] require the use of Gaussian functions, rather than the Slater type used in ADF. Therefore, the geometries of the three complexes were again optimized, both at the HF and MP2 level, using GAMES-US [20] and different basis sets. The technical details about the calculations are given in Section 4. In Fig. 1, we show the two compounds for which a structure is available, containing the cationic complexes, and the MP2 optimized geometry of three models used in the calculations, where phosphines were modeled by PH_3 and the aminopyridine in the neutral complex by $NHCH_2NH_2$.

In Table 1, we give the relevant distances and angles obtained from the HF and the MP2 calculation for the three compounds. In order to avoid repetition, we shall include the results obtained in the absence of the counterion for *cis*-[IrH(OH)$(PH)_4$][PF_6] only. The agreement between the calculated and experimental values is not so good as that obtained in the previous work (see also Table 1) [11], especially in what concerns the HF results, but the main trends are observed. The reason may be the lower quality of the basis sets, which are compatible with our resources when running MP2 calculations. HF gives too long distances for Ir–P and H···H distances. Ir–H bonds are shorter. The influence of the counterion in determining the structure of the cation is clearly shown for **2**, the H···H distance being the most affected, as well as the H–Ir–O angle. They come closer to the experimental value.

The binding energies were calculated for the two cationic species with the geometry shown in Fig. 1 and with either the O–H group (**2**) or the pyrazole ring (**3**) rotated 180°, as shown in Fig. 2 for [$IrH_2(CO)$-$(PPh_3)_2$(pzH–N)][BF_4] (**3**).

The energy differences are high (11.0 kcal mol^{-1} in **2**, 12.5 kcal mol^{-1} in **3**), although the electrostatic contribution should be almost the same (the ions are positioned at the same distance), reflecting mainly the changes in hydrogen bonds, and emphasizing the extra stabilization provided by the anion. For **2**, the O–H···F bonds disappear, and for **3** the N–H···F interaction is replaced by a weaker C–H···F interaction in the less favored conformation. This rotation also destroys the

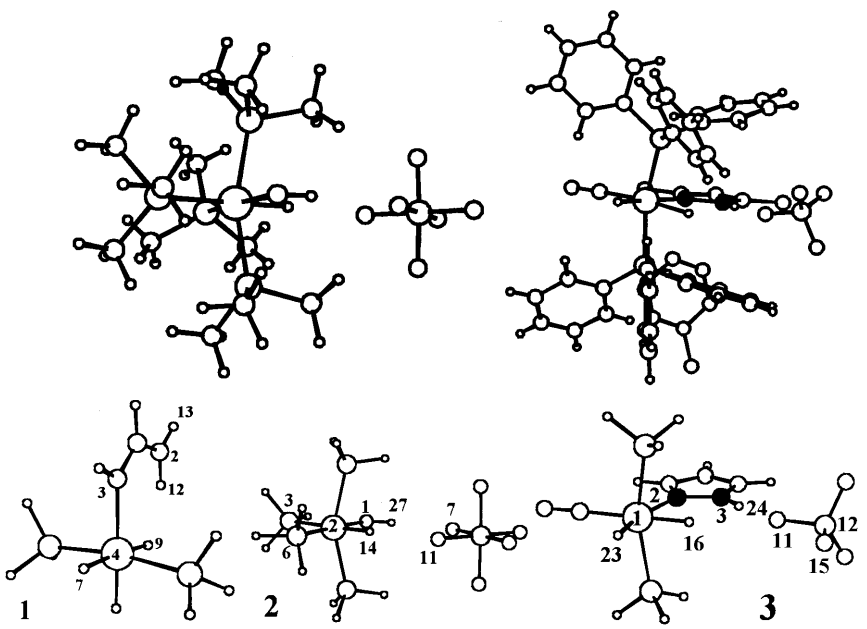

Fig. 1. Experimental geometries of the two compounds *cis*-[IrH(OH)$(PMe)_4$][PF_6] (top, left), [$IrH_2(CO)(PPh_3)_2$(pzH–N)][BF_4](top, right), and calculated geometries of the three models [$Ir(H)_3(PH_3)(NHCH_2NH_2)$] (**1**), *cis*-[IrH(OH)$(PH)_4$][PF_6] (**2**), and [$IrH_2(CO)(PPh_3)_2$(pzH–N)][BF_4] (**3**) (from MP2 optimization).

Table 1
Relevant geometrical parameters from HF and MP2 calculations for $[Ir(H)_3(PH_3)(NHCH_2NH_2)]$ (**1**), *cis*-$[IrH(OH)(PH)_4]^+$ (**2**$^+$), *cis*-$[IrH(OH)(PH)_4][PF_6]$ (**2**), and $[IrH_2(CO)(PPh_3)_2(pzH–N)][BF_4]$ (**3**) (distances/Å, angles/°)

		Ir–H [a]	X–H	Ir–P [b]	H···H	H–Ir–X	P_{ax}–Ir–P_{ax}	Ir–X–H
1	HF	1.702 1.614 1.684	1.002	2.373	1.929	–	170.8	–
	MP2	1.710 1.619 1.691	1.030	2.331	1.818	–	171.7	–
2$^+$	HF	1.596	0.952	2.431 2.563 2.459	2.717	93.8	163.6	119.7
	MP2	1.620	0.987	2.386 2.482 2.389	2.603	92.2	163.0	111.3
	DFT [c]	1.580	0.964	2.285 2.361 2.263	2.470	90.5	180.0 [d]	108.5
2	HF	1.588	0.955	2.425 2.560 2.449	2.543	89.1	158.6	116.8
	MP2	1.619	0.991	2.382 2.473 2.379	2.484	89.1	157.1	109.2
	DFT [c]	1.572	0.969	2.281 2.332 2.243	2.361	88.3	157.5	106.8
	Experiment	1.610	0.922	2.336 2.364 2.352	2.365	86	160	105
3	HF	1.610 1.605	1.012	2.408	2.053	–	160.3	–
	MP2	1.667 1.615	1.044	2.385	2.059	–	159.3	–
	DFT [c]	1.583 1.561	1.043	2.268	2.107		164.1	
	Experiment	1.654 1.663	0.951	2.324 2.336	2.007	–	160	–

[a] The first value refers to the hydride near H–X.
[b] The first value refers to the axial phosphines.
[c] From Ref. [11].
[d] Fixed angle.

M–H···H–X arrangement. A calculation performed in the isolated cation **3**$^+$, where only this interaction was present, shows that the energy increases by 0.9 kcal mol^{-1} only; a much smaller value than those given above.

For the neutral complex, the N–H···H–Ir arrangement can be broken by rotating the N–H group 90° out-of-plane, as already done in the original paper [4b]. In our conditions, this value, which is a crude estimate, was calculated, without further optimization as 29.6 kcal mol^{-1}, compared with 14.42 kcal mol^{-1} in Ref. [4b] (where a geometry optimization was performed).

These equilibrium geometries were used in subsequent calculations. The effect of the basis set was checked on the neutral complex and with RHF calculations, as the size is smaller (no counterion). The best approach was then taken for the study of **2** and **3**. However, the size prevents using the larger and better basis sets with MP2 (see Section 4 for more details).

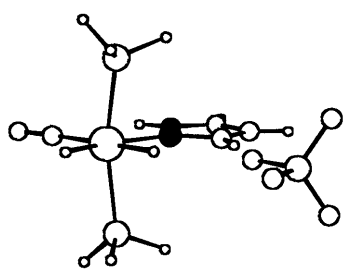

Fig. 2. The geometry of $[IrH_2(CO)(PPh_3)_2(pzH–N)][BF_4]$ (**3**) avoiding any interaction between N–H and the BF_4^- anion.

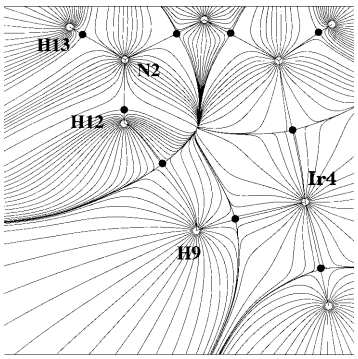

Fig. 3. Gradient of the charge density, $\nabla\rho$, for $[Ir(H)_3(PH_3)(NHCH_2NH_2)]$ in the Ir–H···H–N plane.

Table 2
Charge density ρ and $\nabla^2\rho$ for some bond critical points of $[Ir(H)_3(PH_3)(NHCH_2NH_2)]$ (**1**)

Type of bond	HF		MP2	
	ρ	$\nabla^2\rho$	ρ	$\nabla^2\rho$
H9···H12	0.016	0.041	0.022	0.044
N–H12	0.344	−2.111	0.313	−1.675
N–H13	0.357	−1.974	0.331	−1.640

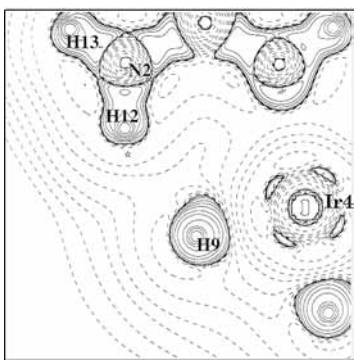

Fig. 4. The laplacian of the charge density $\nabla^2\rho$ in the Ir–H···H–N plane of $[Ir(H)_3(PH_3)(NHCH_2NH_2)]$. Solid lines correspond to $\nabla^2\rho < 0$ (regions of charge concentration) and dashed lines to $\nabla^2\rho > 0$ (regions of charge depletion).

*2.2. The AIM approach — the neutral complex $[Ir(H)_3(PH_3)(NHCH_2NH_2)]$ (**1**)*

The AIM approach [16] relies on an analysis of the topological properties of the charge density $\rho(r)$ and its quality depends on the computational level chosen. Both the gradient and the laplacian of the charge density, $\nabla\rho$ and $\nabla^2\rho$, respectively, can be analyzed and provide complementary information on bonds. The critical points of $\nabla\rho$ give information about the existence of bonds, while the sign of $\nabla^2\rho$ at that point reflects the kind of interaction, namely the laplacian of the charge density, $\nabla^2\rho$, is negative at the critical point for covalent interactions (between open shells), and is positive for closed shell interactions, such as hydrogen bonds. Nuclei attract the charge density so that maxima of ρ are found there. A bond corresponds to a saddle point (the bond critical point), where $\nabla\rho$ becomes zero: a maximum only in one plane of space, and is found joining two trajectories of maximum ρ along the space, towards the nuclei [16].

The plot of the gradient of the charge density $\nabla\rho$ in the plane of the Ir–H···H–N interaction is given in Fig. 3 (HF calculation). The numbering is as shown in Fig. 1.

There are critical bonds between each set of two atoms defining a covalent bond and another one between the hydride H9 and the NH(12). We show, in Table 2, the features of the most relevant critical points, namely for the hydrogen bond, H9···H12, and for the N–H bonds (N–H12, involved in the hydrogen bond and N–H13).

The values of ρ show that there is a much larger charge density in the covalent bonds (two orders of magnitude) than in the hydrogen bond. The laplacian is positive for the hydrogen bond and negative for the two covalent bonds. This method allows the identification of the bond. The comparison between the last two rows in Table 2 shows that the two formerly identical N–H bonds of the complex become different because the hydrogen in one of them is involved in the hydrogen bond. There is less charge density in this bond (N–H12).

Another way of looking at the bonds is shown in Fig. 4, where a map of the laplacian of the charge density $\nabla^2\rho$ in the Ir–H···H–N plane is plotted. The regions of charge concentration (solid lines) can be taken as analogues of the electron pairs in a Lewis structure.

The covalent bonds are found along the direction of maximum charge density, joining the nuclei, as can be checked by looking not only at the N–H bonds discussed above, but also at the others (N–C, N–Ir, Ir–H), in agreement with the values of $\nabla^2\rho$ from Table 2. The H2···H9 hydrogen bond has a different appearance (the critical point in the laplacian is given by the star in the plot), as it corresponds to a minimum of the charge density in a region of charge depletion (positive $\nabla^2\rho$).

Table 2 also contains the characteristics of bonds critical points calculated with MP2. The differences are small, the trends being exactly the same. The plots corresponding to those of Figs. 3 and 4 are also very similar. For this reason, and considering the inherent difficulties, only HF calculations were used in the later analysis of the cationic species.

*2.3. The AIM approach — cis-$[IrH(OH)(PH)_4][PF_6]$ (**2**) and $[IrH_2(CO)(PPh_3)_2(pzH–N)][BF_4]$ (**3**)*

The plot of the gradient of the charge density $\nabla\rho$ in the plane of the Ir–H···H–X interaction is given in Fig.

5 (RHF calculation) for *cis*-[IrH(OH)$(PH)_4$][PF_6] (**2**) and [$IrH_2(CO)(PPh_3)_2$(pzH–N)][BF_4] (**3**), respectively.

The most striking features of both plots is the absence of critical points between the hydrides and the H–X hydrogen, respectively H14···H27 in **2**, and H16···H24 in **3**. This suggests that there is apparently no hydrogen bond. On the other hand, there are several hydrogen bonds involving the fluorides of the counterions, some expected, some unexpected. Before a detailed analysis, we can look at the values of ρ and $\nabla^2\rho$ in Table 3 to help to identify the bonds, following the ideas used above.

These results indicate that there are weak H···F hydrogen bonds in both compounds. While it is not surprising to have them for the N–H···F or O–H···F arrangement, it is unusual to see an Ir–H making not only one, but two hydrogen bonds of the type Ir–H···F in complex **2**. Although the charges in the atoms were not listed, the calculated charges fit the expected values, namely hydrides (H14 in **2**, H16 in **3**) carry negative charges (-0.080, -0.052), while the protonic hydrogens attached to N or O (H27 in **2**, H24 in **3**) are positive (0.333, 0.421), and fluorine is always negative (in all calculations; those involved in hydrogen bonds: F7, -0.610; F11, -0.613; F11, -0.582, respectively for **2** and **3**). It can be thought that the position of the PF_6 anion was constrained, but that is the position it occupies in the structure determined experimentally. The other values given in Table 3 for the covalent bonds are for mainly comparison of the charge density (larger value) and its laplacian (negative).

3. Conclusions

The AIM method appears to be quite helpful for identifying bonds and trying to understand them. Studies available in the literature deal with classic hydrogen bonds, and are not easily comparable with our results involving weaker bonds [16]. In the three compounds studied, the conclusion is that a short H···H distance in a M–H···H–X arrangement is not in itself a diagnostic for a hydrogen bond, of the dihydrogen type. From our calculation (see also Ref. [11]), there is a dihydrogen bond in the neutral complex, but there appears to be no hydrogen bond in the cationic species. The counterion is determining for the final geometry and helps to position the cation. The electrostatic interaction overcomes any weak hydrogen bond that might be formed. As this small sample studied consists of iridium derivatives, the errors in calculations should be similar. Other neutral complexes in the same conditions, for which the

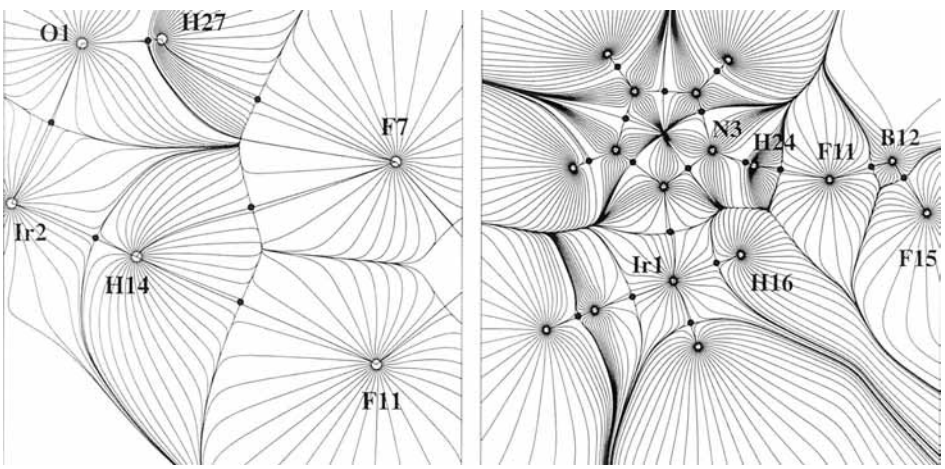

Fig. 5. Gradient of the charge density, $\nabla\rho$, for *cis*-[IrH(OH)$(PH)_4$][PF_6] (**2**, left) and [$IrH_2(CO)(PPh_3)_2$(pzH–N)][BF_4] (**3**, right) in the Ir–H···H–X plane.

Table 3
Charge density ρ and $\nabla^2\rho$ for some bond critical points of *cis*-[IrH(OH)$(PH)_4$][PF_6] (**2**) and [$IrH_2(CO)(PPh_3)_2$(pzH–N)][BF_4] (**3**)

Bond	*cis*-[IrH(OH)$(PH)_4$][PF_6]		Bond	[$IrH_2(CO)(PPh_3)_2$(pzH–N)][BF_4]	
	ρ	$\nabla^2\rho$		ρ	$\nabla^2\rho$
O1–H27	0.380	−2.890	N3 − H24	0.316	−2.247
H27···F7	0.001	0.008	H24···F11	0.030	0.119
H14···F7	0.002	0.009			
H14···F11	0.002	0.010			

structure is available, are more difficult to model and study [11,8]. We decided to keep two cationic species, owing to very different H···H distances. While in the Milstein derivative, *cis*-[IrH(OH)$(PH)_4$][PF_6], it is relatively long and there might be a discussion about any interaction, it goes to less than 2 Å in [IrH_2(CO)-$(PPh_3)_2$(pzH–N)][BF_4] and this is well within the accepted range. These conclusions parallel those from our earlier study and demonstrate the usefulness of the AIM approach to interpret bonds.

4. Experimental

All quantum mechanical computations were effected with the GAMESS-US program [20]. A small modification of the original code was made to allow printing of the natural orbitals (MP2) in a format suitable to be analyzed by the AIM programs.

The geometries were optimized at the RHF and MP2 with and without the presence of the counterion. A symmetry plane defined by the atoms in the hydrogen bond Ir–H···H–X (X = N, O) was considered. Besides making the calculations faster, the AIM analysis becomes much easier to understand. The experimental geometries were simplified by replacing the bulky methyl and phenyl substituents of the phosphines by hydrogen atoms, and C_5H_4NHR by $NHCH_2NH_2$. The influence of the counterion was investigated by performing the geometry optimizations in the presence of the counterion, constrained to be fixed at the experimental position. Effective core potentials (ecp) of Hay and Wadt were used to describe iridium and phosphorus atoms in the ab initio geometry optimizations. For the transition metal centers, the outermost core orbitals, which correspond to ns^2np^6 configurations, were treated explicitly along with the *n*d, (*n* + 1)s and (*n* + 1)p valence orbitals [21]. The Dunning–Hay double ζ split valence basis set was used to describe hydrogen, fluorine, oxygen, sulfur, carbon and nitrogen atoms [22].

The atoms in molecules computations were effected with the AIMPAC suite of programs [19]. It is well known that the ecp basis provides a poor description of the charge density and its associated properties. In order to overcome these problems, the methodology suggested by Frenking et al. was employed [23]. It consists of adding the core orbitals determined from a calculation with an all-electron basis set, while keeping the valence orbitals of the ecp basis. In this work, the simplest implementation consisting of adding the two sets of orbitals without orthogonalization was employed. Preliminary computations where the core functions were added to the basis set used for geometry optimization produced wrong results, specially concerning the identification of the charge depletion area in the valence shell charge concentration of the protonic hydrogen. Instead of having a (3, −3) critical point in $\nabla^2\rho$, the Extreme program of AIMPAC found a (3, −1) critical point. In order to solve this problem, larger basis sets were used for C, N, O, F, B, and H: a Dunning–Hay split valence basis set augmented by two polarization and one diffuse functions, and a 6-311G basis set augmented by one polarization and one diffuse function. For Ir and P, the same basis set was used, but the core functions were added, instead of having them described by pseudopotentials, as in the geometry optimizations. It was shown that both basis sets for light elements produced identical results. Single point runs were done at the RHF level with the RHF geometries. The plots and results shown in this work were obtained with the second set (6-311G). An AIM analysis was also performed with MP2 calculations and the geometry obtained in the MP2 optimization. A different methodology was used to introduce the core electrons. A single point MP2 run was carried out for the MP2 optimized geometry of the neutral [$Ir(H)_3(PH_3)$(NH-CH_2NH_2)] model, with the all-electron minimal basis set of Huzinaga for Ir and P, and a 6-311G basis set augmented by one polarization and one diffuse function for the other atoms [24].

Acknowledgements

This work was partly supported by PRAXIS XXI (PRAXIS/PCNA/C/QUI/103/96). We thank S.F. Vyboishchikov and G. Frenking for their help in making AIM plots when calculations employed effective core potentials.

References

[1] T.R. Richardson, S. Gala, R.H. Crabtree, J. Am. Chem. Soc. 117 (1995) 12875.
[2] (a) D. Milstein, J.C. Calabrese, I.D. Williams, J. Am. Chem. Soc. 108 (1986) 6387. (b) R.C. Stevens, R. Bau, D. Milstein, O. Blum, T.F. Koetzle, J. Chem. Soc. Dalton Trans. (1990) 1429.
[3] J.C. Lee Jr., A.L. Rheingold, B. Muller, P.S. Pregosin, R.H. Crabtree, J. Chem. Soc. Chem. Commun. (1994) 1021.
[4] (a) J.C. Lee Jr., E. Peris, A.L. Rheingold, R.H. Crabtree, J. Am. Chem. Soc. 116 (1994) 110145. (b) E. Peris, J.C. Lee Jr., J.R. Rambo, O. Eisenstein, R.H. Crabtree, J. Am. Chem. Soc. 117 (1995) 3485.
[5] (a) S. Park, R. Ramachandran, A.J. Lough, R.H. Morris, J. Chem. Soc. Chem. Commun. (1994) 2201. (b) A.J. Lough, S. Park, R. Ramachandran, R.H. Morris, J. Am. Chem. Soc. 116 (1994) 8356. (c) W. Xu, A.J. Lough, R.H. Morris, Can. J. Chem. 75 (1997) 475.
[6] (a) J. Wessel, J.C. Lee Jr., E. Peris, G.P.A. Yap, J.B. Fortin, J.S. Ricci, G. Sini, A. Albinati, T.F. Koetzle, O. Eisenstein, A.L. Rheingold, R.H. Crabtree, Angew. Chem. Int. Ed. Engl. 34 (1995) 2507. (b) B.P. Patel, W. Yao, G.P.A. Yap, A.L. Rheingold, R.H. Crabtree, Chem. Commun. (1996) 991. (c) J.C. Lee

Jr., W. Yao, R.H. Crabtree, H. Rüegger, Inorg. Chem. 35 (1996) 695. (d) B.P. Patel, K. Kavallieratos, R.H. Crabtree, J. Organomet. Chem. 528 (1997) 205. (e) R. Bosque, F. Maseras, O. Eisenstein, B.P. Patel, W. Yao, R.H. Crabtree, Inorg. Chem. 36 (1997) 5505. (f) D.-H. Lee, B.P. Patel, E. Clot, O. Eisenstein, R. Crabtree, Chem. Commun. (1999) 297.

[7] (a) R.H. Crabtree, P.E.M. Siegbahn, O. Eisenstein, A.L. Rheingold, T.F. Koetzle, Acc. Chem. Res. 29 (1996) 348. (b) R.H. Crabtree, O. Eisenstein, G. Sini, E. Peris, J. Organomet. Chem. 567 (1998) 7. (c) R.H. Crabtree, J. Organomet. Chem. 577 (1998) 111.

[8] F.H. Allen, J.E. Davies, J.J. Galloy, O. Johnson, O. Kennard, C.F. Mcrae, D.G. Watson, J. Chem. Inf. Comput. Sci. 31 (1991) 204.

[9] (a) T.B. Richardson, T.F. Koetzle, R.H. Crabtree, Inorg. Chim. Acta 250 (1996) 69. (b) E.S. Shubina, N.V. Belkova, L.M. Epstein, J. Organomet. Chem. 536 (1997) 17.

[10] D. Braga, P. DeLeonardis, F. Grepioni, E. Tedesco, M.J. Calhorda, Inorg. Chem. 37 (1998) 3337.

[11] D. Braga, F. Grepioni, E. Tedesco, M.J. Calhorda, P.E.M. Lopes, New J. Chem. 23 (1999) 219.

[12] (a) Q. Liu, R. Hoffmann, J. Am. Chem. Soc. 117 (1995) 10108. (b) N.V. Belkova, E.S. Shubina, A.V. Ionidis, L.M. Epstein, H. Jacobsen, A. Messmer, H. Berke, Inorg. Chem. 36 (1997) 1522. (c) G. Orlova, S. Scheiner, J. Phys. Chem. 102 (1998) 260. (d) G. Orlova, S. Scheiner, J. Phys. Chem. 102 (1998) 4813.

[13] A.L. Bandini, G. Banditelli, F. Bonati, G. Minghetti, F. Demartin, M. Manassero, Inorg. Chem. 26 (1987) 1351.

[14] C. Moller, M.S. Plesset, Phys. Rev. 46 (1934) 618.

[15] (a) P. Pyykkö, Chem. Rev. 97 (1997) 524. (b) P. Pyykkö, in: D. Braga, F. Grepioni, A.G. Orpen (Eds.), Crystal Engineering: From Molecules to Crystals to Materials, Kluwer Academic, Dordrecht, 1999 and references therein. (c) E. Ruiz, D.R. Salahub, A. Vela, J. Phys. Chem. 100 (1996) 12265. (d) A.C. Cooper, E. Clot, J.C. Huffman, W.E. Streib, F. Maseras, O. Eisenstein, K.G. Caulton, J. Am. Chem. Soc. 121 (1999) 97.

[16] (a) R.F.W. Bader, Atoms in Molecules — A Quantum Theory, Oxford Science, Oxford, 1990. (b) R.F.W. Bader, Chem. Rev. 91 (1991) 893. (a) M.T. Carroll, C. Chang, R.F.W. Bader, Mol. Phys. 63 (1988) 387. (b) M.T. Carroll, R.F.W. Bader, Mol. Phys. 65 (1988) 695. (d) R.G.A. Bone, R.F.W. Bader, J. Phys. Chem. 100 (1996) 10892. (e) http://www.chemistry.mcmaster.ca/faculty/bader/aim. (f) I. Alkorta, I. Rozas, J. Elguero, Theor. Chem. Acc. 99 (1998) 116.

[17] R.G. Parr, W. Yang, Density Functional Theory of Atoms and Molecules, Oxford University, New York, 1989.

[18] Amsterdam density functional (ADF) program, release 2.3, Vrije Universiteit, Amsterdam, The Netherlands, 1995.

[19] F.W. Bieger-Konig, R.F. Bader, T.-H. Tang, J. Comp. Chem. 3 (1982) 317.

[20] M.W. Schmidt, K.K. Baldridge, J.A. Boatz, S.T. Elbert, M.S. Gordon, J.J. Jensen, S. Koseki, N. Matsunaga, K.A. Nguyen, S. Su, T.L. Windus, M. Dupuis, J.A. Montgomery, J. Comp. Chem. 14 (1993) 1347.

[21] (a) P.J. Hay, W.R. Wadt, J. Chem. Phys. 82 (1985) 271. (b) W.R. Wadt, P.J. Hay, J. Chem. Phys. 82 (1985) 284.

[22] T.H. Dunning, P.J. Hay, in: H.F. Schaeffer (Ed.), Methods of Electronic Structure Theory, vol. 2, Plenum, New York, 1977.

[23] (a) Z. Lin, I. Bytheway, Inorg. Chem. 35 (1996) 594. (b) S.F. Vyboishchikov, A. Sierralta, G. Frenking, J. Comp. Chem. 18 (1997) 416.

[24] S. Huzinaga, J. Andzelm, M. Klobukowski, E. Radzio-Andzelm, Y. Sakai, H. Tatewaki, Gaussian Basis Sets for Molecular Calculations, Elsevier, Amsterdam, 1984.